PROCEEDINGS OF SCIENCE

NNLO contributions to ε_K and rare kaon decays

Martin Gorbahn[*] [†]
Technische Universität München, Institute for Advanced Study,
Arcisstraße 21, D-80333 München, Germany
E-mail: martin.gorbahn@ph.tum.de

We discuss the theory prediction of ε_K and the rare $K \to \pi\nu\bar{\nu}$ decays and review the structure and current status of higher-order contributions to these flavour changing processes in the standard model in some detail. This includes the next-to-next-to-leading order QCD calculation to the charm quark contribution to $K^+ \to \pi^+\nu\bar{\nu}$ and to the charm-top quark contribution to ε_K. Electroweak corrections to the rare kaon decays are also discussed.

2009 KAON International Conference KAON09,
June 09 - 12 2009
Tsukuba, Japan

[*]Speaker.
[†]Martin Gorbahn enjoys the hospitality of the Excellence Cluster "Origin and Structure of the Universe."

1. Introduction

Rare decays of K-mesons as well as K^0-$\overline{K^0}$ mixing continue to play an important role in fixing parameters of the standard model (SM) and in constraining models of new physics. In the future ε_K, the parameter describing indirect CP violation in kaon mixing, and the decays $K^+ \to \pi^+ \nu\bar{\nu}$, $K_L \to \pi^0 \nu\bar{\nu}$ will provide a decisive test of the SM and its extensions: they are highly sensitive to new physics [1] and their theory prediction is under good control for ε_K and remarkably clean for $K \to \pi\nu\bar{\nu}$. In the SM these modes are dominated by internal top quark contributions proportional to powers of $V_{ts}^* V_{td}$ and as such are suppressed with respect to generic new physics scenarios by the near diagonality of the Cabibbo-Kobayashi-Maskawa (CKM) matrix. Also these modes can be calculated precisely using an effective theory framework. The matrix elements are extracted from K_{l3} decays for $K \to \pi\nu\bar{\nu}$ [2], and from the lattice for ε_K [3]. This leads to an exceptionally clean prediction for the rare $K \to \pi\nu\bar{\nu}$ decays, while the recent and expected progress for the lattice calculations of $\hat{B}_K$, the bag parameter for ε_K, is quite remarkable.

2. Structure of $K \to \pi\nu\bar{\nu}$ at NLO

The theoretical cleanness of the $K \to \pi\nu\bar{\nu}$ decays in the SM is related to the quadratic Glashow-Iliopoulos-Maiani (GIM) mechanism. Using $\lambda_i = V_{is}^* V_{id}$ and $x_i = m_i^2/M_W^2$ we can write the amplitude of the Z-penguin and electroweak box diagrams (Fig. 1) as

$$\begin{aligned} &\lambda_t \left(F(x_t) - F(x_u)\right) + \lambda_c \left(F(x_c) - F(x_u)\right) = \\ &\mathcal{O}\left(\lambda^5 \frac{m_t^2}{M_W^2}\right) \qquad + \left[\mathcal{O}\left(\lambda \frac{m_c^2}{M_W^2}\right) \ln \frac{m_c}{M_W} + \mathcal{O}\left(\lambda \frac{\Lambda_{\rm QCD}^2}{M_W^2}\right) \ln \frac{m_c}{M_W}\right]. \end{aligned} \tag{2.1}$$

Here $\lambda_t F(x_t)$ is the top quark contribution, which is suppressed by five powers of the Cabibbo angle $\lambda = |V_{\rm us}|$, and $\lambda_c F(x_c)$ is the charm quark contribution. The contribution of soft internal up quarks is suppressed by $\Lambda_{\rm QCD}^2/M_W^2$.

Related to the quadratic GIM mechanism is the fact that the low-energy effective Hamiltonian

$$\mathscr{H}_{\rm eff} = \frac{4G_F}{\sqrt{2}} \frac{\alpha}{2\pi \sin^2\theta_W} \sum_{l=e,\mu,\tau} \left(\lambda_c X^l(x_c) + \lambda_t X(x_t)\right) (\bar{s}_L \gamma_\mu d_L)(\bar{\nu}_{lL} \gamma^\mu \nu_{lL}) \tag{2.2}$$

involves only one single operator $Q_\nu = (\bar{s}_L \gamma^\mu d_L)(\bar{\nu}_L \gamma_\mu \nu_L)$. The hadronic matrix element of the low-energy effective Hamiltonian can be extracted from the well-measured K_{l3} decays, including isospin breaking and long-distance QED radiative corrections.

The anomalous dimension of the operator in (2.2) vanishes. Hence the top quark contribution in (2.1) has no large logarithm and is calculated in fixed-order perturbation theory. The matching of the electroweak box and Z-penguin diagrams in Fig. 1 with internal charm quarks gives the charm quark contribution to the Wilson coefficient of Q_ν. Next, one matches Green's functions with internal W- and Z-Bosons and dimension-six current-current operators. The bilocal mixing into the dimension-eight operator $m_c^2 Q_\nu$ – see Fig. 1 – resums the large logarithm in (2.1). The GIM mechanism cancels all loop contributions which do not carry an explicit charm mass dependence. Only when integrating out the charm quark higher-dimensional operators appear. The matching

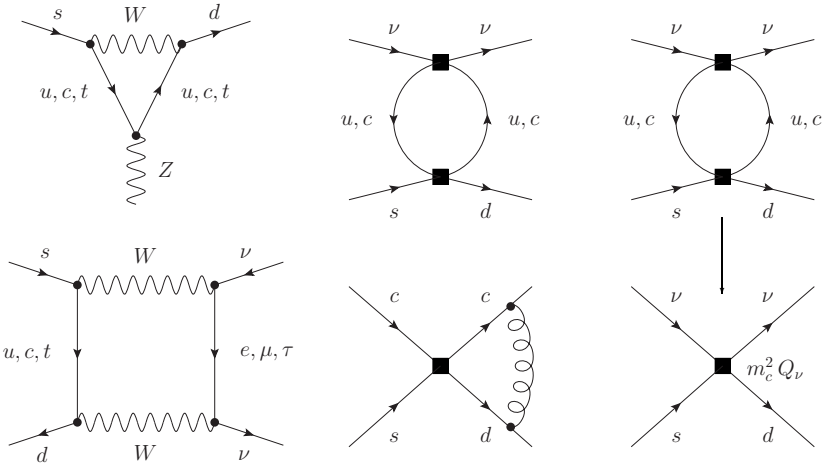

Figure 1: Left column: The Z-penguin and electroweak box give the matching contribution to the charm and top sector. Middle column: The mixing of the current-current operators into $m_c^2 Q_\nu$ and the self-mixing of the current-current operators. Right column: Integrating out the charm quark produces $m_c^2 Q_\nu$ and subleading higher dimensional operators.

onto Q_ν in Fig. 1 gives the dominant contribution to the branching ratio, while the contribution of the higher-dimensional operators can be computed together with the matrix element containing soft up quarks with the help of chiral perturbation theory (χPT) [4].

After extracting the matrix element of Q_ν from K_{l3} decays and summation over the three neutrino flavours the resulting branching ratio for $K \to \pi\nu\bar{\nu}$ can be written as [4, 5, 6]

$$\begin{aligned}\mathscr{B}(K^+ \to \pi^+\nu\bar{\nu}) &= \kappa_+ (1+\Delta_{\rm EM}) \left[\left(\frac{{\rm Im}\lambda_t}{\lambda^5} X(x_t) \right)^2 + \left(\frac{{\rm Re}\lambda_t}{\lambda^5} X(x_t) + \frac{{\rm Re}\lambda_c}{\lambda} \left(P_c + \delta P_{c,u} \right) \right)^2 \right] , \\ \mathscr{B}(K_L \to \pi^0\nu\bar{\nu}) &= \kappa_L \left(\frac{{\rm Im}\lambda_t}{\lambda^5} X(x_t) \right)^2 .\end{aligned} \tag{2.3}$$

Here $\kappa_+ = 0.5173(25) \times 10^{-10} (\lambda/0.225)^8$ and $\kappa_L = 2.231(13) \times 10^{-10} (\lambda/0.225)^8$ contain higher-order electroweak corrections for the normalisation to the K_{l3} decays, and $\Delta_{\rm EM} \simeq -0.3\%$ denotes long distance QED corrections [6]. The top quark $X(x_t) = 1.464 \pm 0.041$, computed at two-loop in Ref. [7], gives the only contribution to $\mathscr{B}(K_L \to \pi^0\nu\bar{\nu})$, while its contribution to $\mathscr{B}(K^+ \to \pi^+\nu\bar{\nu})$ is 63%. The perturbative part of the charm quark contribution at NLO [7] is

$$P_c^{\rm NLO} = 0.364 \pm 0.036_{\rm theory} \pm 0.009_{m_c} \pm 0.009_{\alpha_s} , \tag{2.4}$$

for $\lambda = 0.2255$. The parametric uncertainty – see Ref. [8] for input parameters – is small compared to the theoretical error, which results from higher order corrections. In a χPT calculation [4] the contribution of higher dimensional operators and soft up quarks has been calculated to $\delta P_{c,u} = 0.04 \pm 0.02$. Using Eq. (2.3), Eq. (2.4), and the input parameters of Ref. [8] results in:

$$\begin{aligned}\mathscr{B}(K^+ \to \pi^+\nu\bar{\nu})^{\rm NLO} &= (8.5 \pm 0.5_{\rm sd} \pm 0.2_{\rm ld} \pm 0.6_{\rm param}) \times 10^{-11} , \\ \mathscr{B}(K_L \to \pi^0\nu\bar{\nu})^{\rm NLO} &= (2.7 \pm 0.1_{\rm sd} \pm 0.04_{\rm ld} \pm 0.4_{\rm param}) \times 10^{-11} .\end{aligned} \tag{2.5}$$

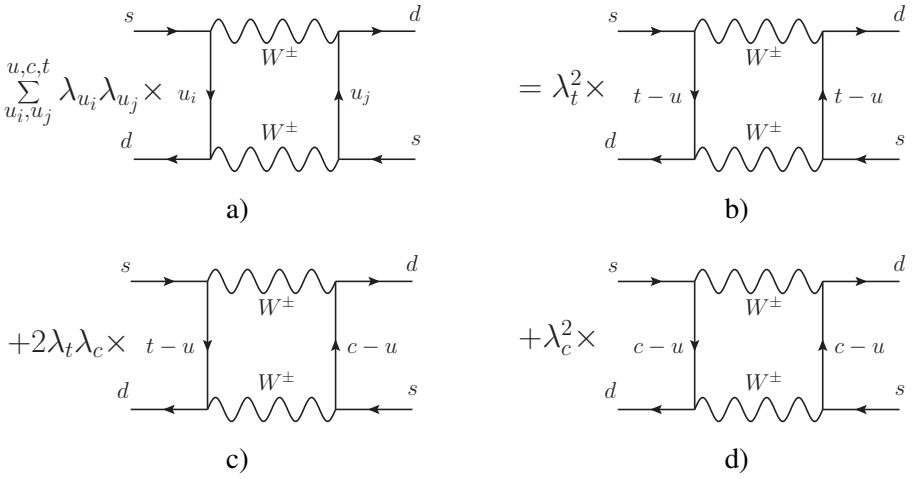

Figure 2: The $\Delta S = 2$ Box-type diagram with internal up, charm, and top contributions is expressed as a sum of Box-type diagrams proportional to λ_t^2, λ_c^2, and $\lambda_t\lambda_c$ respectively using the GIM mechanism.

The subscript "sd", "ld", and "param" labels the perturbative, long-distance, and parametric uncertainties respectively. The parametric error is dominated by the CKM parameters, while $\delta P_{c,u}$ gives the largest contribution to the long-distance uncertainty of the charged decay mode.

3. Structure of ε_K at NLO

The parameter

$$\varepsilon_K = \frac{\mathscr{A}\left(K_L \to (\pi\pi)_{I=0}\right)}{\mathscr{A}\left(K_S \to (\pi\pi)_{I=0}\right)} \tag{3.1}$$

measures CP violation in K_0–$\overline{K_0}$ mixing via the ratio of the respective decay amplitudes of a K_L and a K_S decaying into a two pion state of isospin zero. Its generic structure shares features with the previously discussed $K \to \pi\nu\bar{\nu}$ decays: only one operator $Q_{S2} = (\bar{s}\gamma_\mu d_L)(\bar{s}\gamma_\mu d_L)$ contributes dominantly below the charm quark mass scale and long-distance effects are power suppressed, this time because of CP violation.

For the theoretical prediction it is useful to express ε_K in terms of $\langle K^0|\mathscr{H}_{eff}^{\Delta S=2}|\bar{K}^0\rangle = 2m_K M_{12}^*$, the matrix element of the $\Delta S = 2$ effective Hamiltonian, and write:

$$\varepsilon_K = e^{i\phi_\varepsilon}\sin\phi_\varepsilon\left(\frac{\mathrm{Im}(M_{12}^*)}{\Delta M_K} + \xi\right). \tag{3.2}$$

Here the phase of ε_K is $\phi_\varepsilon = 43.5(7)^\circ$ [9] and $\xi = \mathrm{Im}A_0/\mathrm{Re}A_0 \simeq 0$ is the imaginary part divided by the real part of the isospin zero amplitude $A_0 = \mathscr{A}\left(K_S \to (\pi\pi)_{I=0}\right)$. The ratio $\kappa_\varepsilon = |\varepsilon_K^{SM}/\varepsilon_K(\phi_\varepsilon = 45^\circ, \xi = 0)|$ encompasses the change of $|\varepsilon_K|$ if the values $\phi_\varepsilon = 45^\circ$ and $\xi = 0$ are used in (3.2), as has been done in most of the older analyses, instead of the exact values. The authors of Ref. [10] used ε'/ε to extract the value of $\kappa_\varepsilon = 0.92 \pm 0.02$ in the SM.

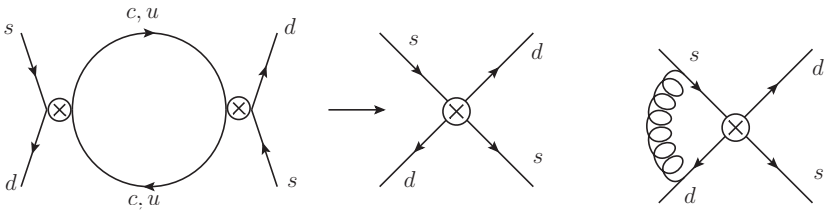

Figure 3: Dimension 6 current-current and penguin operators mix at LO into Q_{S2} with a CKM factor proportional to $\lambda_t\lambda_c$ in a). Integrating out the charm quark results in similar diagrams for the LO and NLO matching of the contribution proportional to $\lambda_t\lambda_c$ and λ_c^2 respectively. A sample diagram which is relevant to the LO evolution of Q_{S2} is shown in b).

The box diagram of Fig. 2a gives the leading contribution to the $\Delta S = 2$ effective Hamiltonian and the parameter M_{12}. It is proportional to a sum of loop functions times CKM factors:

$$\sum_{u_i,u_j\in\{u,c,t\}} \lambda_{u_i}\lambda_{u_j}\tilde{S}(\frac{m_{u_i}^2}{M_W^2},\frac{m_{u_j}^2}{M_W^2}) = \lambda_t^2 S(x_t) + \lambda_c^2 S(x_c) + \lambda_t\lambda_c S(x_t,x_c)\ . \tag{3.3}$$

After the GIM mechanism has been used to eliminate $\lambda_u = -\lambda_t - \lambda_c$ it comprises the top quark contribution – proportional to λ_t^2 (Fig. 2b), the charm quark contribution – proportional to λ_c^2 (Fig. 2c), and the charm-top quark contribution (Fig. 2d) – proportional to $\lambda_t\lambda_c$. The resulting loop functions $S(x_i,x_j) = \tilde{S}(x_i,x_j) - \tilde{S}(x_i,0) - \tilde{S}(0,x_j) + \tilde{S}(0,0)$ and $S(x_i) = S(x_i,x_i)$ are suppressed by the smallness of the quark mass m_i if $x_i = m_i^2/M_W^2$ is significantly smaller than one. This, together with the severe Cabibbo suppression of the CP violating top quark contribution, lets all three contributions compete in size for ε_K:

$$\mathrm{Im}\left(\lambda_t^2 S(x_t) + \lambda_c^2 S(x_c) + \lambda_t\lambda_c S(x_t,x_c)\right) \simeq \mathscr{O}\left(\lambda^{10}\right) + \mathscr{O}\left(\lambda^6\frac{m_c^2}{M_W^2}\right)\ln\left(\frac{m_c}{M_W}\right) + \mathscr{O}\left(\lambda^6\frac{m_c^2}{M_W^2}\right)\ . \tag{3.4}$$

The diagram of Fig. 2a induces a large logarithm ($\ln m_c/M_W$) only for the charm-top quark contribution: the large logarithm from the up-quarks in Fig. 2b is power suppressed by $\Lambda_{\mathrm{QCD}}^2/M_W^2$, while the GIM mechanism cancels a potential $\ln m_c/M_W$ between the diagrams with both one up and one charm quark and the diagram with only internal charm quarks.

This can be reformulated in an effective theory language: the dimension-six penguin as well as the current-current operators, which have tree-level Wilson coefficients, mix only into the charm-top quark contribution, via the bilocal mixing in Fig. 3a, yet do not induce large logarithms times tree-level Wilson coefficients proportional to λ_t^2 and λ_c^2. QCD corrections do not change this picture but only induce the well known RGE effects for the $\Delta S = 1$ effective Hamiltonian [11] and for the $\Delta S = 2$ Operator Q_{S2} (Fig. 3b). A LO analysis of the charm quark and top quark contribution to ε_k then requires a one-loop calculation both for the matching at μ_W, for the running, and for the matching of the charm quark contribution also for the matching at μ_c (Fig. 3a). This is contrary to the charm-top quark contribution where a tree-level matching at μ_W and μ_c is sufficient at LO.

After integrating out the charm quark the $\Delta S = 2$ effective Hamiltonian reads

$$\mathscr{H}_{\mathrm{eff}}^{\Delta S=2} = \frac{G_F^2}{4\pi^2}M_W^2\left[\lambda_c^2\eta_{\mathrm{cc}}S(x_c) + \lambda_c^2\eta_{\mathrm{tt}}S(x_t) + \lambda_c^2\eta_{\mathrm{ct}}S(x_c,x_t)\right]b(\mu)Q_{S2} + \mathrm{h.c.} + \ldots \tag{3.5}$$

where the QCD and logarithmic corrections are known at NLO and parametrised by $\eta_{cc} = 1.43(23)$ [12], $\eta_{ct} = 0.47(4)$ [12], and $\eta_{tt} = 0.5765(65)$ [13]. The parameter $b(\mu)$ is factored out such that

$$\hat{B}_K = \frac{3}{2} b(\mu) \frac{\langle K^0 | Q_{S2} | \overline{K^0} \rangle}{f_K^2 m_K^2} \tag{3.6}$$

is a renormalisation group invariant quantity, which can be calculated on the lattice – see e.g. [14] and Ref.[3] of this conference. Using $\hat{B}_K = 0.720 \pm 0.013 \pm 0.037$ one finds for ε_K at NLO [10]:

$$\varepsilon_K^{\rm NLO} = (1.78 \pm 0.25)\,, \tag{3.7}$$

where η_{tt}, η_{ct}, and η_{cc} contribute with 75%, 37%, and -12% respectively to the total value of ε_K, while 60% of the uncertainty is of parametric origin and 40% is of theoretical origin. The parametric error is dominated by the uncertainty in the CKM parameters, while the perturbative and non-perturbative uncertainties are comparable in size for the theory uncertainty.

Finally note that $\mathscr{H}^{\Delta S=2}$ also contains higher dimensional Operators in $\mathscr{H}^{\Delta S=2}_{\rm eff,d=8}$ and current-current operators with up-quarks in $\mathscr{H}^{\Delta S=1}_{\rm eff,up}$, as indicated by the ellipses in Eq. (3.5). At leading order in the $1/N_C$ expansion only one higher-dimensional operator is present and its matrix element is estimated in [15] to result in a 0.5% enhancement of ε_K.

4. NNLO QCD corrections

The NNLO calculation of ε_K and $K^+ \to \pi^+ \nu\bar{\nu}$ aims at resumming all $\mathscr{O}(\alpha_s^n \ln^{n-1}(\mu_W^2/\mu_c^2))$ logarithms for P_c and η_{ct} and all $\mathscr{O}(\alpha_s^n \ln^{n-2}(\mu_W^2/\mu_c^2))$ for $X(x_t)$, η_{tt}, and η_{cc}. The theory uncertainty of P_c and η_{ct} dominates the perturbative error for $K^+ \to \pi^+ \nu\bar{\nu}$ and ε_K respectively at NLO, while the large theory uncertainty in η_{cc} is somewhat suppressed by the smallness of the charm contribution to ε_K.

A NNLO analysis for P_c and η_{ct} will reduce the theory uncertainties and comprises (i) the $\mathscr{O}(\alpha_s^2)$ matching corrections to the relevant Wilson coefficients arising at μ_W, (ii) the $\mathscr{O}(\alpha_s^3)$ anomalous dimensions describing the mixing of the dimension-six and the Q_ν and Q_{S2} operators, (iii) the $\mathscr{O}(\alpha_s^2)$ threshold corrections to the Wilson coefficients originating at μ_b, and (iv) the $\mathscr{O}(\alpha_s^2)$ matrix elements of the operators emerging at μ_c. To determine the contributions of type (i), (iii), and (iv) one must calculate two-loop Green functions in the full SM and in effective theories with five or four flavours. Sample diagrams for steps (i) and (iv) are shown in the left and right columns of Fig. 4. The contributions (ii) are found by calculating three-loop Green functions with operator insertions. Sample diagrams with a double insertion of dimension-six operators are shown in the centre column of Fig. 4. The corresponding three-loop amplitudes are evaluated using the method that has been described in [11, 16]. A comprehensive discussion of the technical details of the matching, the renormalisation of the effective theory and the actual calculation is given in [5] for the calculation of P_c and will be given in [17] for the calculation of η_{ct}. The same techniques have also been used to reduce the uncertainties in the short-distance contribution to $K_L \to \mu^+\mu^-$ [18].

The aforementioned QCD calculation results for the input parameters of Ref. [8] in the following value for P_c at NNLO:

$$P_c^{\rm NNLO} = 0.368 \pm 0.009_{\rm theory} \pm 0.009_{m_c} \pm 0.009_{\alpha_s}\,. \tag{4.1}$$

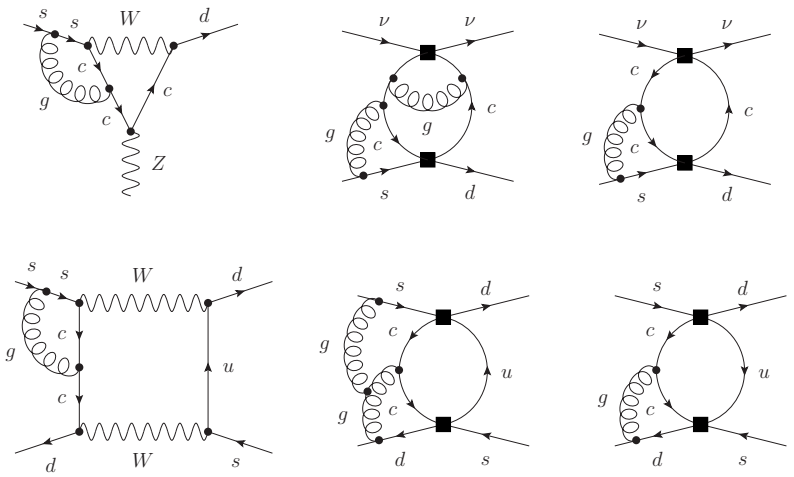

Figure 4: Examples of Feynman diagrams arising in the full SM (left column), describing the mixing of operators (centre column) and the matrix elements (right column) for the Z-penguin sector of $K^+ \to \pi^+ \bar{\nu}\nu$ (upper row) and for ε_K (lower row). Only the divergent pieces of the diagrams displayed in the centre column have to be computed, while the Feynman graphs shown on the left- and right-hand side are needed including their finite parts.

Comparing these numbers with Eq. (2.4) we observe that the NNLO calculation reduces the theoretical uncertainty by a factor of 4. Because of this and the improvement in the calculation of long-distance effects [2], unknown electroweak corrections could potentially dominate the theory uncertainty of the rare $K \to \pi\nu\bar{\nu}$ decays. Even though a similar reduction of the error for $\eta_{\rm ct}$ is expected at NNLO in QCD [17] no electroweak corrections are needed for the present theoretical status of ε_K.

5. Electroweak corrections

The NLO calculation of electroweak corrections for rare $K \to \pi\bar{\nu}\nu$ decays resums all LO and NLO logarithmic QED corrections and fixes the scheme electroweak input parameters, like $\sin^2\theta_W$, by an electroweak matching calculation. The function P_c depends on the charm quark $\overline{\rm MS}$ mass through the parameter x_c, conventionally defined as $x_c = m_c^2/M_W^2$. The point of fixing the input parameters can be exemplified by noting that the charm quark contribution is mediated by a double insertion of two dimension-six operators. This results in a contribution of $\mathcal{O}(G_F^2)$ – the second power of G_F resides in x_c – plus electroweak corrections. Yet the leading result of Eq. (2.2) can only approximate the electroweak corrections for a specific choice of the renormalisation scheme for the prefactor of the charm quark contribution, expressed as $\alpha/\sin^2\theta_W$. While it is expected that using $\overline{\rm MS}$ parameters renormalised at the electroweak scale would approximate the electroweak corrections best [19], only an explicit calculation can provide a definite result. We normalise all dimension-six operators to G_F and replace the parameter x_c with the definition

$$x_c = \sqrt{2}\frac{\sin^2\theta_W}{\pi\alpha} G_F m_c^2(\mu_c)\,, \tag{5.1}$$

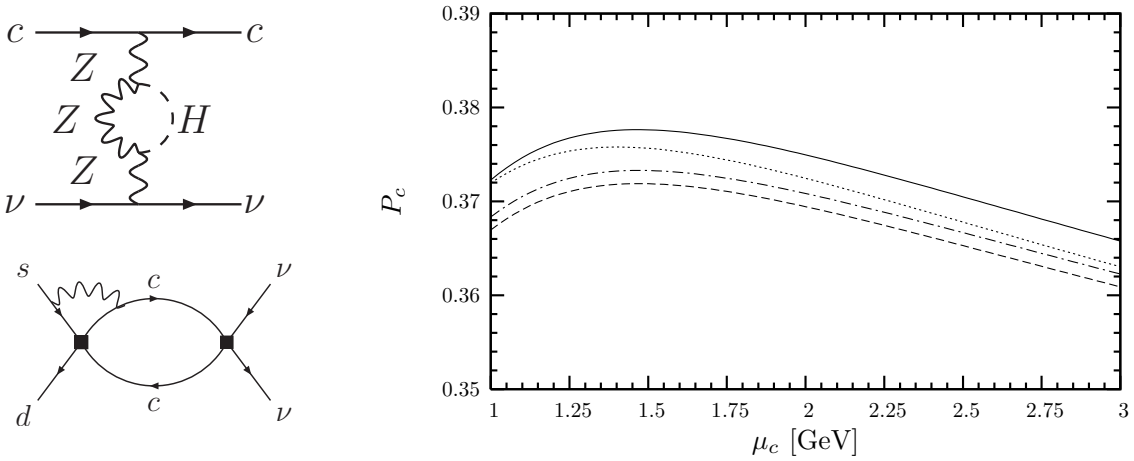

Figure 5: Left column: Example of a diagram describing the NLO matching to a dimension-six operator involving charm quarks and neutrinos (top) and of a diagram contributing to the NLO mixing of two dimension-six operators into Q_ν. Right column: $P_c(X)$ as a function of μ_c at NNLO QCD (dashed dotted line), including LO QED (dotted line), and NLO electroweak corrections (solid line). The dashed line shows $P_c(X)$ at NNLO QCD where the definition $x_c = m_c^2/M_W^2$ is used.

which only at tree level equals the ratio $m_c^2(\mu_c)/M_W^2$.

The NLO analysis of electroweak effects of Ref. [8] involves the calculation of one-loop matching corrections for the dimensions-six operators (top left diagram of Fig. 5) and QED corrections to the LO QCD operator mixing (bottom left diagram of Fig. 5), and the inclusion of QED effects in the expansion of the matrix elements at μ_c. Note that the LO QED corrections start at $\mathcal{O}(\alpha^2 \ln^2(\mu_W^2/\mu_c^2))$ while the first NLO electroweak correction is $\mathcal{O}(\alpha^2 \ln(\mu_W^2/\mu_c^2))$. This explains why $P_c(x)$, which is plotted on the right column of Fig. 5 as a function of the parameter μ_c, receives corrections of similar size. Also the cancellation of the scheme dependence between the LO QED and the NLO electroweak contribution is clearly visible and we see that including the full electroweak corrections, $P_c(X)$ is mildly increased as compared to the pure NNLO QCD. The number for the branching ratio then reads [8]:

$$\mathcal{B}\left(K^+ \to \pi^+ \nu\bar{\nu}\right) = (8.51^{+0.57}_{-0.62\,\mathrm{CKM}} \pm 0.20_{m_c,m_t,\alpha_s} \pm 0.36_{\mathrm{theory}}) \times 10^{-11}\,. \tag{5.2}$$

The CKM parameters dominate the parametric uncertainty. The main contributions to the theory error stem from the uncertainty in $\delta P_{c,u}$ and X_t, where we used an error of 2%. In detail, the contributions to the theory error are ($\kappa_\nu^+ : 6\%$, $X_t : 38\%$, $P_c : 17\%$, $\delta P_{c,u} : 39\%$), respectively. All errors have been added in quadrature.

6. Conclusions

Rare $K \to \pi\nu\bar{\nu}$ decays and the CP violating parameter ε_K are extremely sensitive to flavour violating new physics. The good control of long-distance contribution to these observables makes the calculation of NNLO QCD and sometimes even NLO electroweak corrections mandatory. Results for NNLO QCD and NLO electroweak corrections for the charm quark contributions to rare

K decays have been published in Ref. [5, 8], while the NNLO calculation of the charm-top quark contribution is finished [17]. This, together with current [20] and future [21] progress from the experimental side, will increase the new physics reach of these observables further.

Acknowledgments

I would like to thank the organisers of the KAON09 conference for the invitation to such an interesting meeting. A big thank you to J. Brod for his careful reading of this manuscript.

References

[1] P. Paradisi, PoS(KAON09)044.

[2] C. Smith, PoS(KAON09)010.

[3] P. Boyle, PoS(KAON09)002.

[4] G. Isidori, F. Mescia and C. Smith, Nucl. Phys. B **718**, 319 (2005).

[5] A. J. Buras, M. Gorbahn, U. Haisch, and U. Nierste, Phys. Rev. Lett. **95**, 261805 (2005); A. J. Buras, M. Gorbahn, U. Haisch, and U. Nierste, [arXiv:hep-ph/0603079].

[6] F. Mescia and C. Smith, Phys. Rev. D **76** (2007) 034017 [arXiv:0705.2025 [hep-ph]].

[7] G. Buchalla and A. J. Buras, Nucl. Phys. B **412**, 106 (1994), M. Misiak and J. Urban, Phys. Lett. B **451** (1999) 161 [arXiv:hep-ph/9901278], G. Buchalla and A. J. Buras, Nucl. Phys. B **548**, 309 (1999);

[8] J. Brod and M. Gorbahn, Phys. Rev. D **78** (2008) 034006 [arXiv:0805.4119 [hep-ph]].

[9] C. Amsler *et al.* [Particle Data Group], Phys. Lett. B **667** (2008) 1.

[10] A. J. Buras and D. Guadagnoli, Phys. Rev. D **79** (2009) 053010 [arXiv:0901.2056 [hep-ph]].

[11] M. Gorbahn and U. Haisch, Nucl. Phys. B **713**, 291 (2005).

[12] S. Herrlich and U. Nierste, Nucl. Phys. B **419** (1994) 292 [arXiv:hep-ph/9310311]; S. Herrlich and U. Nierste, Phys. Rev. D **52** (1995) 6505 [arXiv:hep-ph/9507262]; S. Herrlich and U. Nierste, Nucl. Phys. B **476** (1996) 27 [arXiv:hep-ph/9604330].

[13] A. J. Buras, M. Jamin and P. H. Weisz, Nucl. Phys. B **347**, 491 (1990).

[14] D. J. Antonio *et al.* [RBC Collaboration and UKQCD Collaboration], Phys. Rev. Lett. **100** (2008) 032001 [arXiv:hep-ph/0702042]; C. Allton *et al.* [RBC-UKQCD Collaboration], Phys. Rev. D **78** (2008) 114509 [arXiv:0804.0473 [hep-lat]]; C. Aubin, J. Laiho and R. S. Van de Water, arXiv:0905.3947 [hep-lat].

[15] O. Cata and S. Peris, JHEP **0407** (2004) 079 [arXiv:hep-ph/0406094].

[16] K. G. Chetyrkin, M. Misiak and M. Münz, Nucl. Phys. B **518**, 473 (1998); P. Gambino, M. Gorbahn and U. Haisch, Nucl. Phys. B **673**, 238 (2003).

[17] J. Brod and M. Gorbahn, in preparation; J. Brod, PhD Thesis, Karlsruhe, 2009;

[18] M. Gorbahn and U. Haisch, Phys. Rev. Lett. **97** (2006) 122002 [arXiv:hep-ph/0605203].

[19] C. Bobeth, P. Gambino, M. Gorbahn and U. Haisch, JHEP **0404** (2004) 071 [arXiv:hep-ph/0312090].

[20] J. K. Ahn [E391a Collaboration], arXiv:hep-ex/0607016.

[21] G. Ruggiero, PoS(KAON09)043; H. Nanjo, PoS(KAON09)047; D. A. Bryman, PoS(KAON09)049.